5. ECOLOGICAL IMPACTS OF THE 2015/16 EL NIÑO IN THE CENTRAL EQUATORIAL PACIFIC

Russell E. Brainard, Thomas Oliver, Michael J. McPhaden, Anne Cohen, Roberto Venegas, Adel Heenan, Bernardo Vargas-Ángel, Randi Rotjan, Sangeeta Mangubhai, Elizabeth Flint, and Susan A. Hunter

Coral reef and seabird communities in the central equatorial Pacific were disrupted by record-setting sea surface temperatures, linked to an anthropogenically forced trend, during the 2015/16 El Niño.

Introduction. In the equatorial Pacific Ocean, the El Niño–Southern Oscillation substantially affects atmospheric and oceanic conditions on interannual time scales. The central and eastern equatorial Pacific fluctuates between anomalously warm and nutrient-poor El Niño and anomalously cool and nutrient-rich La Niña conditions (Chavez et al. 1999; McPhaden et al. 2006; Gierach et al. 2012). El Niño events are characterized by an eastward expansion of the Indo-Pacific warm pool (IPWP) and deepening of the thermocline and nutricline in response to weakening trade winds (Strutton and Chavez 2000; Turk et al. 2001). El Niño events are typically associated with significant decreases in primary productivity in the eastern and central tropical Pacific and corresponding increases in productivity in the western tropical Pacific (Boyce et al. 2010).

The IPWP has warmed and expanded in recent decades (Weller et al. 2016). The eastern Pacific cold tongue, on the other hand, has exhibited signs of a cooling trend over the past century (Deser et al. 2010). Newman and Wittenberg (2018) found that anomalously warm sea surface temperatures (SST) in the Niño-4 region (5°N–5°S, 150°E–150°W) of the central equatorial Pacific (CEP) during the 2015/16 El Niño were likely unprecedented and unlikely to have occurred naturally, thereby reflecting an anthropogenically forced trend. Lee and McPhaden (2010) earlier reported increasing amplitudes of El Niño events in Niño-4 that is also evident in our study region (Figs. 5.1b,c).

Remote islands in the CEP (Fig. 5.1a), including Jarvis Island (0°22′S, 160°01′W), Howland Island (0°48′N, 176°37′W), Baker Island (0°12′N, 176°29′W), and Kanton Island (2°50′S, 171°40′W), support healthy, resilient coral reef ecosystems characterized by exceptionally high biomass of planktivorous and piscivorous reef fishes due to the combined effects of equatorial and topographic upwelling (Gove et al. 2006; Williams et al. 2015). Coral reef communities at these islands are exposed to extended periods of thermal stress during El Niño events. Mass coral bleaching and mortality were reported in the Phoenix Islands during the moderate 2002/03 El Niño (Obura and Mangubhai 2011), and coral bleaching with limited mortality was reported at Howland and Baker Islands during the moderate 2009/10 El Niño (Vargas-Ángel et al. 2011). There were no observations of coral bleaching or mortality at these uninhabited islands during the major El Niño events of 1982/83 or 1997/98. Corals in the eastern equatorial Pacific (>7600 km to the east) did experience mass bleaching and mortality during those major El Niño events (Glynn 1984; Glynn et al. 2001).

We describe variations in SST and biological productivity to characterize the 2015/16 El Niño (McPhaden 2015) in relation to previous El Niño events in the CEP (Fig. 5.1a) and in the context of climate trends. We then describe some of the ecological responses, which were catastrophic at Jarvis and modest at Howland, Baker, and Kanton Islands.

Data and methods. The duration and magnitude of El Niño events for the period 1981–2017 for our region of interest (ROI; 5°N–5°S, 150°W–180°) were identified

AFFILIATIONS: Brainard—NOAA Pacific Islands Fisheries Science Center, Ecosystem Sciences Division, Honolulu, Hawaii; Oliver, Venegas, Heenan, and Vargas-Ángel—University of Hawaii, Joint Institute for Marine and Atmospheric Research, Honolulu, and NOAA Pacific Islands Fisheries Science Center, Ecosystem Sciences Division, Honolulu, Hawaii; McPhaden—NOAA Pacific Marine Environmental Laboratory, Seattle, Washington; Cohen—Woods Hole Oceanographic Institution, Woods Hole, Massachusetts; Rotjan—Boston University, Boston, Massachusetts; Mangubhai—Wildlife Conservation Society, Suva, Fiji; Flint and Hunter—U.S. Fish and Wildlife Service, Marine National Monuments of the Pacific, Honolulu, Hawaii

DOI:10.1175/BAMS-D-17-0128.1

A supplement to this article is available online (10.1175/BAMS-D-17-0128.2)

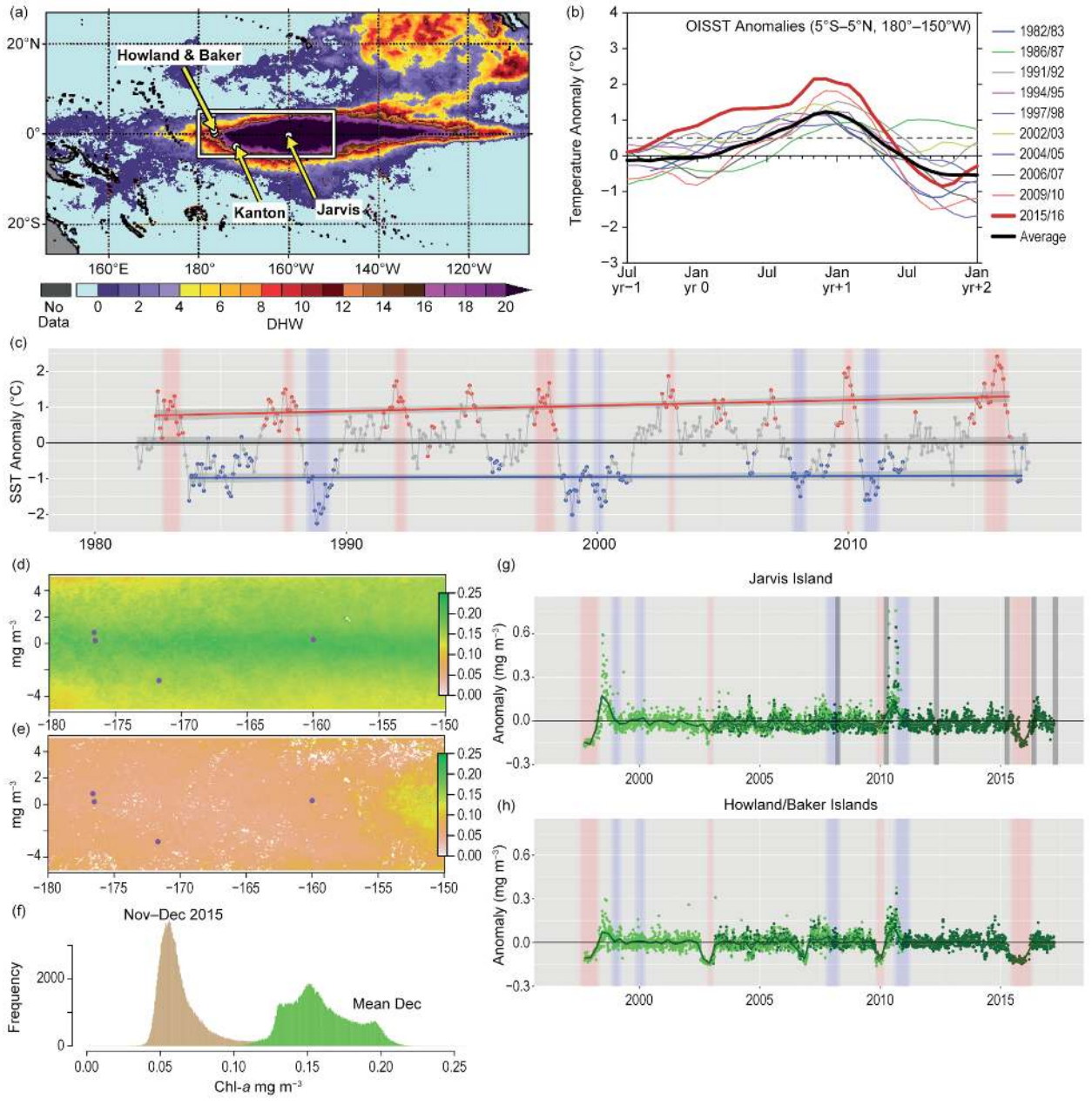

Fig. 5.1. (a) NOAA Coral Reef Watch 5-km degree heating weeks for the Pacific Ocean for 1 Jan 2016 (https://coralreefwatch.noaa.gov/satellite/bleaching5km/images_archive/b05kmnn_dhw_20160101_pacific_930x580.gif) overlaid with ROI boundaries and locations of Jarvis, Howland, Baker, and Kanton Islands. (b) ROI SST anomalies (°C) for El Niño events since 1981 based on OISST data. Thick black line is average of all events since 1981 excluding the 2015/16 event. Thick red line is Jul 2014–Jan 2017, encompassing the 2015/16 El Niño. (c) Time series of monthly OISST anomaly (°C) for ROI; El Niño and La Niña periods are shown as vertical red and blue bands, respectively. Trends for El Niño, neutral, and La Niña conditions are shown as red, gray, and blue lines. (d) Map of mean Chl-*a* (mg m^{-3}) for all Dec from 2002–16 for ROI using MODIS data showing strong equatorial upwelling; (e) mean Chl-*a* (mg m^{-3}) for Nov–Dec 2015 for ROI using MODIS data showing 'desertification' conditions; (f) frequency of occurrences of Chl-*a* (mg m^{-3}) concentrations over the ROI for Dec mean over 2003–17 (green) and Nov–Dec 2015 (tan); (g) time series of Chl-*a* (mg m^{-3}) anomalies at Jarvis Island (2° × 2°; 0.63°N–1.37°S, 159°–161°W) from SeaWiFS (1997–2010) and MODIS (2003–17) datasets https://coastwatch.pfeg.noaa.gov/erddap, (h) time series of Chl-*a* anomalies (mg m^{-3}) at Howland/Baker Islands (2° × 2°; 1.5°N–0.5°S, 175.5°–177.5°W) from SeaWiFS and MODIS datasets.

using the NOAA 1/4° daily optimum interpolation SST (OISST; online supplement material). El Niño or La Niña events were defined following the convention for the ONI index, that is, when the 3-month running mean SST anomaly in Niño-3.4 exceeded ±0.5°C. We computed trends during El Niño, La Niña, and neutral conditions during the El Niño events. We examined long-term trends of SST anomaly and cumulative heat stress in the ROI and at Jarvis Island using OISST, the NOAA extended reconstructed SST (ERSSTv4; Huang et al. 2014), and Hadley Centre sea ice and SST dataset (HadISST; online supplement material). To identify the location and variations in primary biological productivity, estimates of chlorophyll concentration (Chl-*a*) were obtained from SeaWiFS (9-km) from 1997–2010 and MODIS (4-km) from 2002–17 (NASA 2014; online supplement material).

From 2000–17, coral reef benthic and fish communities were surveyed during 11 research cruises by NOAA's Pacific Reef Assessment and Monitoring Program. The cruise monitoring data were used to examine the ecological responses to recent El Niño events. Surveys included visual estimates of coral cover (%) collected during towed-diver surveys at mid-depths (~15 m) from 2001–17 (Kenyon et al. 2006) and visual estimates from stratified random benthic surveys since 2010. Fish assemblages were surveyed since 2008 using a stationary point count method under a random depth-stratified sampling design (Ayotte et al. 2015). Changes in seabird populations were based on visual surveys conducted immediately before and after the 1982/83 and 2015/16 El Niño events and using fixed cameras that captured images every 30 minutes from April 2015 to May 2016.

Results and discussion: Oceanographic patterns. Exceptionally warm SST anomalies for the ROI (Figs. 5.1b,c) and Jarvis Island (Figs. ES5.1b,c) show that the 2015/16 El Niño was the strongest in magnitude and longest on record in the satellite era. Though SST was also anomalously warm in the CEP for extended durations during other major El Niño events in 1982/83, 1997/98, 2009/10, the warming at Jarvis Island during the 2015/16 El Niño was exceptional. Observed daily SST anomalies exceeded the 1982/83, 1997/98, and 2009/10 events by +0.51°, +0.52°, and +0.71°C, respectively (difference among events of 95% quantiles of daily SST; Figs. ES5.1b,c). At Howland and Baker Islands, ~1830 km west of Jarvis Island, the 2015/16 El Niño showed SST maxima on par with the 2009/10 event, but exceeded levels observed in 1982/83 and 1997/98 by +0.61° and +0.68°C, respectively (Fig. ES5.1d). SST anomalies were substantially smaller at Howland and Baker Island than at Jarvis Island for all events, by 0.42° to 1.28°C, respectively.

Time series of daily OISST anomalies during El Niño events show statistically significant warming trends of +0.596° (0.166°C decade^{-1}) and +0.352° (0.098°C decade^{-1}) over 36 years in the ROI and at Jarvis Island, respectively (Figs. 5.1c and ES5.1b). This trend is robust to the exclusion of 2015/16 El Niño across the ROI, but not at Jarvis Island alone (Table ES5.1). Combining magnitude and duration of SST anomalies using the ERRSTv4 and HadISST reconstructions since 1950, cumulative heat stress during El Niño periods demonstrates warming trends of +0.43° (0.064°C decade^{-1}) and +0.50° (0.074°C decade^{-1}) over the past 67 years in the ROI and at Jarvis Island, respectively (Figs. ES5.4a,b; Table ES5.2), though again, the significance of this warming trend depends on the inclusion of the 2015/16 El Niño. With the observed warming trend in the IPWP (Weller et al. 2016), it appears that the significant warming across the CEP, including Jarvis Island, during El Niño events may be due to eastward advection of these increasingly warmer waters.

During strong El Niño events, a cessation of upwelling can lead to extended periods of anomalously low Chl-*a*, as occurred at Jarvis Island during only the strongest El Nino events in 1997/98 and 2015/16 (Fig. 5.1g). At Howland and Baker Islands, low Chl-*a* events were more frequent, occurring during these major El Niño events and the moderate El Niño events of 2002/03 and 2009/10 (Fig. 5.1h). The strong El Niño events of 1982/83 and 1997/98 were followed by strong La Niña events, but this did not occur following the 2015/16 El Niño. La Niña events that followed the 1997/98 and 2009/10 El Niño events were characterized by robust Chl-*a* phytoplankton blooms that lasted ~6 months at Jarvis, Howland, and Baker Islands. Without a strong La Niña following the 2015/16 El Niño, no such Chl-*a* bloom was observed in 2016–17. In summary, primary productivity fluctuated between 'desertification' conditions during strong El Niño events and robust phytoplankton blooms during strong La Niña events (Figs. 5.1e–h).

Ecological responses. The 2015/16 El Niño was a major driver of the longest, most widespread, and most damaging global coral bleaching event on record (NOAA 2017). In the CEP, impacts to corals were catastrophic at Jarvis, but only moderate or modest at Howland, Baker, and Kanton Islands. Specifically, NOAA reported severe coral mortality at Jarvis Island

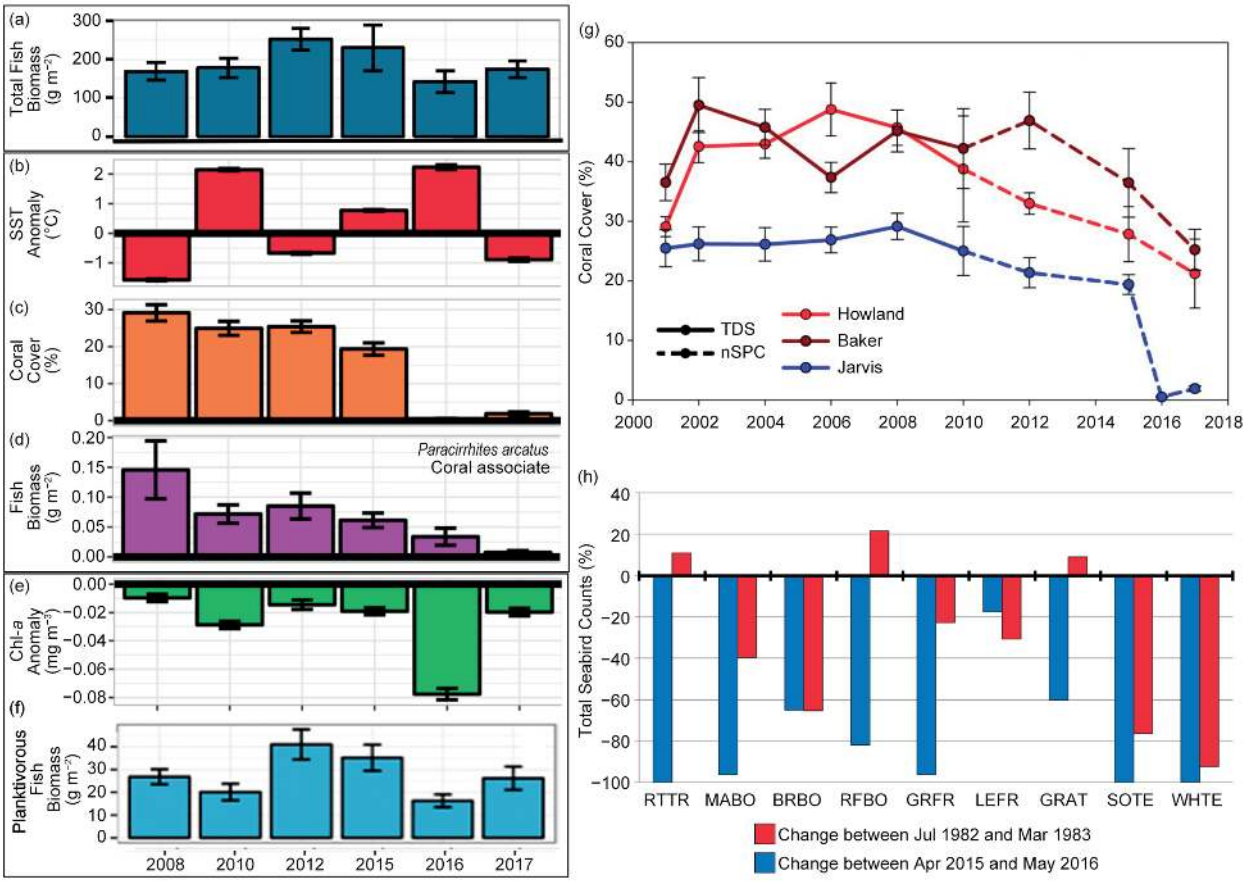

Fig. 5.2. (a)–(f) Jarvis Island. (a) Mean fish biomass (g m^{-2}) and standard error (SE) computed from stratified random reef fish surveys of abundance and size; (b) 6-mo running mean SST anomalies (°C) and SE for 6-mo prior to NOAA fish and coral surveys using OISST; (c) mean coral cover (%) and SE from NOAA towed-diver surveys (2008 only) and stratified random stationary point count (SPC) surveys (2010–17): (d) mean biomass (g m^{-2}) of coral associate *Paracirrhites arcatus*. (e) 6-mo running mean Chl-*a* anomalies (mg m^{-3}) for 6-mo prior to NOAA fish and coral surveys using MODIS. (f) Island-wide mean plantivorous fish biomass (g m^{-2}) and SE computed from stratified random SPC reef fish surveys of abundance and size. (g) Mean coral cover (%) and SE (2001–08 from NOAA towed-diver surveys at mean 15-m depth (solid lines) ; 2010–17 from NOAA stratified random SPC surveys). (h) Change of Jarvis Island seabird counts (%) before and after 1982–83 (blue) and 2015–16 (red) El Niño events. [Data were normalized using census data from 19 island surveys from 1973 to 2016 (x-min. count)/(max.-min.).]; RTTR = *Phaethon rubricauda*; MABO, BRBO, & RFBO = *Sula dactylatra*, *S. leucogaster*, & *S. sula*; GRFR & LEFR = *Fregata minor* & *F. ariel*; GRAT & SOTE = *Onychoprion lunatus* and *O. fuscatus*; WHTE = *Gygis alba*.

with island-wide coral cover declining from 17.8% in April 2015 (pre-bleaching) to 0.3% in May 2016 (post-bleaching), representing a devastating decline of >95% (Fig. 5.2g; Table ES5.3; Boyle et al. 2017; Vargas-Ángel et al. 2017, manuscript submitted to *Coral Reefs*). Corals at Jarvis Island experienced thermal stress of 35.8 degree heating weeks and exceeded the bleaching threshold (28.7°C) for 43 consecutive weeks between 2015 and 2016 (Boyle et al. 2017). Extensive mass bleaching observed visually during the peak of the El Niño in November 2015 (Cohen 2016, personal communication) caused mass mortality across all coral taxa, reef habitats, and depths by May 2016 (Figs. 5.2c,g; Table ES5.3). Only a few hardy and resilient corals survived, including some massive Porites colonies that had survived previous El Niño events over many decades and a few colonies of Acropora, Pocillopora, and Hydnophora (Boyle et al. 2017; Vargas-Ángel et al. 2017, manuscript submitted to *Coral Reefs*).

In contrast, Howland, Baker, and Kanton Islands experienced substantially less thermal stress. At Howland and Baker Islands, we observed 23%–31% reductions in coral cover from 2015 to 2017, though there were no observations to confirm bleaching during the 2015/16 El Niño (Fig. 5.2g; Table ES5.3).

The reduction in coral cover between 2015 and 2017 is smaller than the reduction in coral cover from 2012 to 2015, which was an ENSO neutral period. At Kanton Island, 5%–25% of the corals were observed to be bleached during the peak of the 2015/16 El Niño, but little discernable coral mortality was observed in 2016, dramatically lower than the mortality observed following the 2002/03 El Niño (Mangubhai and Rotjan 2017, personal commmunication; Obura and Mangubhai 2011).

A preliminary assessment of reef fish survey data at Jarvis Island revealed decreased total fish biomass in 2016 relative to other years (Fig. 5.2a; Table ES5.4), consistent with previous findings from the Phoenix Islands following the 2002/03 bleaching (Mangubhai et al. 2014). In addition, biomass of planktivores was lower during both the moderate and strong El Niño events of 2009/10 and 2015/16 (Fig. 5.2f). With the island-wide reduction in coral cover observed since 2008, a concomitant reduction in the biomass of *Parracirrhites arcatus,* a fish species dependent on live coral for habitat, was observed (Figs. 5.2c,d). These combined data suggest that the 2015/16 El Niño caused reduced food availability (Fig. 5.2e) that depleted planktivore populations (Fig. 5.2f) and reduced coral cover (Fig. 5.2c) which in turn reduced live-coral dependent fish species (Fig. 5.2d).

Seabird counts at Jarvis Island showed a decrease in total individuals and a scarcity of older nestlings, indicating a lack of reproduction, after the 2015/16 El Niño (Fig. 5.2h). Wildlife cameras recorded a decrease in birds flying to and from the sea and loss of colonies from flooding events. Nineteen seabird counts from 1973–2016 showed a negative relationship between the abundance of most species and the Niño-3.4 index.

Conclusions. The long-term warming trend in the IPWP has coincided with a corresponding warming trend across the CEP during major El Niño events, culminating in record high SST and Chl-*a* anomalies across the CEP in association with the extreme 2015/16 El Niño that disrupted coral reef and seabird communities, especially at Jarvis Island, where catastrophic coral bleaching and mortality were observed.

ACKNOWLEDGMENTS. The authors thank Cisco Werner (NOAA/NMFS) for proposing this special issue and encouraging our submission. We thank each of the editors, Stephanie Herring, Peter Stott, and Nikos Christidis, for helpful guidance and support throughout the submittal process. We also thank each of the anonymous external reviewers for thoughtful guidance and suggestions to improve the manuscript. REB, TO, RV, AH, and BVA are grateful for support from the NOAA Coral Reef Conservation Program. AC acknowledges support from the National Science Foundation for the following awards: OCE 1537338, OCE 1605365, and OCE 1031971. This is PMEL contribution no. 4698. Any use of trade, firm, or product names is for descriptive purposes only and does not imply endorsement by the U.S. government. The views expressed in the article are not necessarily those of the U.S. government.

REFERENCES

Ayotte, P., K. McCoy, A. Heenan, I. Williams, and J. Zamzow, 2015: Coral Reef Ecosystem Program standard operating procedures: Collection for rapid ecological assessment fish surveys. Pacific Islands Fisheries Science Center Administrative Report H-15-07, 33 pp., doi:10.7289/V5SN06ZT.

Boyce, D. G., M. R. Lewis, and B. Worm, 2010: Global phytoplankton decline over the past century. *Nature*, **466**, 591–596, doi:10.1038/nature09268.

Boyle, S., and Coauthors, 2017: *Coral reef ecosystems of the Pacific Remote Islands Marine National Monument: A 2000–2016 overview.* PIFSC Special Pub. SP-17-003, 62 pp., doi.org/10.7289/V5/SP-PIFSC-17-003.

Chavez, F. P., P. G. Strutton, G. E. Friederich, R. A. Feely, G. C. Feldman, D. G. Foley, and M. J. McPhaden, 1999: Biological and chemical response of the equatorial Pacific Ocean to the 1997–1998 El Niño. *Science*, **286**, 2126–2131, doi:10.1126/science.286.5447.2126.

Deser, C., A. S. Philips, and M. A. Alexander, 2010: Twentieth century tropical sea surface temperature trends revisited. *Geophys. Res. Lett.*, **37**, L10701, doi:10.1029/2010GL043321.

Gierach, M. M., T. Lee, D. Turk, and M. J. McPhaden, 2012: Biological response to the 1997-98 and 2009-2010 El Niño events in the equatorial Pacific Ocean. *Geophys. Res. Lett.*, **39**, L10602, doi:10.1029/2012GL051103.

Glynn, P. W., 1984: Widespread coral mortality and the 1982–83 El Niño warming event. *Environ. Conserv.*, **11**, 133–146, doi:10.1017/S0376892900013825.

——, J. L. Maté, A. C. Baker, and M. O. Calderón, 2001: Coral bleaching and mortality in Panama and Ecuador during the 1997–1998 El Niño–Southern Oscillation event: Spatial/temporal patterns and comparisons with the 1982–1983 event. *Bull. Mar. Sci.*, **69**, 79–109.

Gove, J. M., M. A. Merrifield, and R. E. Brainard, 2006: Temporal variability of current-driven upwelling at Jarvis Island. *J. Geophys. Res.*, **111**, C12011, doi:10.1029/2005JC003161.

Huang, B., and Coauthors, 2014: Extended reconstructed sea surface temperature version 4 (ERSST.v4): Part I. Upgrades and intercomparisons. *J. Climate*, **28**, 911–930, doi:10.1175/JCLI-D-14-00006.1.

Kenyon J., R. Brainard, R. Hoeke, F. Parrish, and C. Wilkinson, 2006: Towed-diver surveys, a method for mesoscale spatial assessment of benthic reef habitat: A case study at Midway Atoll in the Hawaiian Archipelago. *Coastal Manage.*, **34**, 339–349, doi:10.1080/08920750600686711.

Lee, T., and M. J. McPhaden, 2010: Increasing intensity of El Niño in the central equatorial Pacific. *Geophys. Res. Lett.*, **37**, L14603, doi:10.1029/ 2010GL044007.

Mangubhai, S., A. M. Strauch, D. O. Obura, G. Stone, and R. D. Rotjan, 2014: Short-term changes of fish assemblages observed in the near-pristine reefs of the Phoenix Islands. *Rev. Fish Biol. Fish.*, **24**, 505–518, doi:10.1007/s11160-013-9327-5.

McPhaden, M. J., 2015: Playing hide and seek with El Niño. *Nat. Climate Change*, **5**, 791–795, doi:10.1038 /nclimate2775.

——, S. E. Zebiak, and M. H. Glantz, 2006: ENSO as an integrating concept in Earth science. *Science*, **314**, 1740–1745, doi:10.1126/science.1132588.

NOAA, 2017: Global coral bleaching event likely ending. News & Features [online], National Oceanic and Atmospheric Administration. [Available online at www.noaa.gov/media-release/global-coral -bleaching-event-likely-ending.]

Newman, M. and A. Wittenberg, 2018: The extreme 2015/16 El Niño in the context of historical climate variability and change [in "Explaining Extreme Events of 2016 from a Climate Perspective"]. *Bull. Amer. Meteor. Soc.*, **99** (1), S16–S20, doi;10.1175 /BAMS-D-17-0116.1

Obura, D., and S. Mangubhai, 2011: Coral mortality associated with thermal fluctuations in the Phoenix Islands, 2002–2005. *Coral Reefs*, **30**, 607–619, doi:10.1007/s00338-011-0741-7.

Strutton, P. G., and F. P. Chavez, 2000: Primary productivity in the equatorial Pacific during the 1997–998 El Niño. *J. Geophys. Res.,* **105**, 26,089–26,101, doi:10.1029/1999JC000056.

Turk, D., M. J. McPhaden, A. J. Busalacchi, and M. R. Lewis, 2001: Remotely-sensed biological production in tropical Pacific during 1992–1999 El Niño and La Niña. *Science*, **293**, 471–474, doi:10.1126 /science.1056449.

Vargas-Ángel, B., E. E. Looney, O. J. Vetter, and E. F. Coccagna, 2011: Severe, widespread El Niño–associated coral bleaching in the US Phoenix islands. *Bull. Mar. Sci.*, **87**, 623–638.

Weller, E., S.-K. Min, W. Cai, F. W. Zwiers, Y.-H. Kim, and D. Lee, 2016: Human-caused Indo-Pacific warm pool expansion. *Sci. Adv.*, **2**, e1501719, doi:10.1126 /sciadv.1501719.

Williams, I. D., J. K. Baum, A. Heenan, K. M. Hanson, M. O. Nadon, and R. E. Brainard, 2015: Human, oceanographic and habitat drivers of central and western Pacific coral reef fish assemblages. *PLoS One*, **10**, e0120516, doi:10.1371/journal.pone.0120516.

Table 1.1. SUMMARY of RESULTS

ANTHROPOGENIC INFLUENCE ON EVENT			
	INCREASE	**DECREASE**	**NOT FOUND OR UNCERTAIN**
Heat	Ch. 3: Global Ch. 7: Arctic Ch. 15: France Ch. 19: Asia		
Cold		Ch. 23: China Ch. 24: China	
Heat & Dryness	Ch. 25: Thailand		
Marine Heat	Ch. 4: Central Equatorial Pacific Ch. 5: Central Equatorial Pacific Ch. 6: Pacific Northwest Ch. 8: North Pacific Ocean/Alaska Ch. 9: North Pacific Ocean/Alaska Ch. 9: Australia		Ch. 4: Eastern Equatorial Pacific
Heavy Precipitation	Ch. 20: South China Ch. 21: China (Wuhan) Ch. 22: China (Yangtze River)		Ch. 10: California (failed rains) Ch. 26: Australia Ch. 27: Australia
Frost	Ch. 29: Australia		
Winter Storm			Ch. 11: Mid-Atlantic U.S. Storm "Jonas"
Drought	Ch. 17: Southern Africa Ch. 18: Southern Africa		Ch. 13: Brazil
Atmospheric Circulation			Ch. 15: Europe
Stagnant Air			Ch. 14: Western Europe
Wildfires	Ch. 12: Canada & Australia (Vapor Pressure Deficits)		
Coral Bleaching	Ch. 5: Central Equatorial Pacific Ch. 28: Great Barrier Reef		
Ecosystem Function		Ch. 5: Central Equatorial Pacific (Chl-***a*** and primary production, sea bird abundance, reef fish abundance) Ch. 18: Southern Africa (Crop Yields)	
El Niño	Ch. 18: Southern Africa		Ch. 4: Equatorial Pacific (Amplitude)
TOTAL	18	3	9

	METHOD USED	Total Events
Heat	Ch. 3: CMIP5 multimodel coupled model assessment with piCont, historicalNat, and historical forcings Ch. 7: CMIP5 multimodel coupled model assessment with piCont, historicalNat, and historical forcings Ch. 15: Flow analogues conditional on circulation types Ch. 19: MIROC-AGCM atmosphere only model conditioned on SST patterns	
Cold	Ch. 23: HadGEM3-A (GA6) atmosphere only model conditioned on SST and SIC for 2016 and data fitted to GEV distribution Ch. 24: CMIP5 multimodel coupled model assessment	
Heat & Dryness	Ch. 25: HadGEM3-A N216 Atmosphere only model conditioned on SST patterns	
Marine Heat	Ch. 4: SST observations; SGS and GEV distributions; modeling with LIM and CGCMs (NCAR CESM-LE and GFDL FLOR-FA) Ch. 5: Observational extrapolation (OISST, HadISST, ERSST v4) Ch. 6: Observational extrapolation; CMIP5 multimodel coupled model assessment Ch. 8: Observational extrapolation; CMIP5 multimodel coupled model assessment Ch. 9: Observational extrapolation; CMIP5 multimodel coupled model assessment	
Heavy Precipitation	Ch. 10: CAM5 AMIP atmosphere only model conditioned on SST patterns and CESM1 CMIP single coupled model assessment Ch. 20: Observational extrapolation; CMIP5 and CESM multimodel coupled model assessment; auto-regressive models Ch. 21: Observational extrapolation; HadGEM3-A atmosphere only model conditioned on SST patterns; CMIP5 multimodel coupled model assessment with ROF Ch. 22: Observational extrapolation, CMIP5 multimodel coupled model assessment Ch. 26: BoM seasonal forecast attribution system and seasonal forecasts Ch. 27: CMIP5 multimodel coupled model assessment	
Frost	Ch. 29: *weather@home* multimodel atmosphere only models conditioned on SST patterns; BoM seasonal forecast attribution system	
Winter Storm	Ch. 11: ECHAM5 atmosphere only model conditioned on SST patterns	
Drought	Ch. 13: Observational extrapolation; weather@home multimodel atmosphere only models conditioned on SST patterns; HadGEM3-A and CMIP5 multimodel coupled model assessent; hydrological modeling Ch. 17: Observational extrapolation; CMIP5 multimodel coupled model assessment; VIC land surface hdyrological model, optimal fingerprint method Ch. 18: Observational extrapolation; *weather@home* multimodel atmosphere only models conditioned on SSTs, CMIP5 multimodel coupled model assessment	
Atmospheric Circulation	Ch. 15: Flow analogues distances analysis conditioned on circulation types	
Stagnant Air	Ch. 14: Observational extrapolation; Multimodel atmosphere only models conditioned on SST patterns including: HadGEM3-A model; EURO-CORDEX ensemble; EC-EARTH+RACMO ensemble	
Wildfires	Ch. 12: HadAM3 atmospere only model conditioned on SSTs and SIC for 2015/16	
Coral Bleaching	Ch. 5: Observations from NOAA Pacific Reef Assessment and Monitoring Program surveys Ch. 28: CMIP5 multimodel coupled model assessment; Observations of climatic and environmental conditions (NASA GES DISC, HadCRUT4, NOAA OISSTV2)	
Ecosystem Function	Ch. 5: Observations of reef fish from NOAA Pacific Reef Assessment and Monitoring Program surveys; visual observations of seabirds from USFWS surveys. Ch. 18: Empirical yield/rainfall model	
El Niño	Ch. 4: SST observations; SGS and GEV distributions; modeling with LIM and CGCMs (NCAR CESM-LE and GFDL FLOR-FA) Ch. 18: Observational extrapolation; *weather@home* multimodel atmosphere only models conditioned on SSTs, CMIP5 multimodel coupled model assessment	
		30